IOWA STATE UNIVERSITY
Digital Repository

Biochemistry, Biophysics and Molecular Biology Publications | Biochemistry, Biophysics and Molecular Biology

3-2016

AAE13 encodes a dual-localized malonyl-CoA synthetase that is crucial for mitochondrial fatty acid biosynthesis

Xin Guan
Iowa State University

Basil J. Nikolau
Iowa State University, dimmas@iastate.edu

Follow this and additional works at: https://lib.dr.iastate.edu/bbmb_ag_pubs

 Part of the Genetics and Genomics Commons, Molecular Biology Commons, and the Plant Sciences Commons

The complete bibliographic information for this item can be found at https://lib.dr.iastate.edu/bbmb_ag_pubs/322. For information on how to cite this item, please visit http://lib.dr.iastate.edu/howtocite.html.

This Article is brought to you for free and open access by the Biochemistry, Biophysics and Molecular Biology at Iowa State University Digital Repository. It has been accepted for inclusion in Biochemistry, Biophysics and Molecular Biology Publications by an authorized administrator of Iowa State University Digital Repository. For more information, please contact digirep@iastate.edu.

AAE13 encodes a dual-localized malonyl-CoA synthetase that is crucial for mitochondrial fatty acid biosynthesis

Abstract

Malonyl-CoA is a key intermediate in a number of metabolic processes associated with its role as a substrate in acylation and condensation reactions. These types of reactions occur in plastids, the cytosol and mitochondria, and although carboxylation of acetyl-CoA is the known mechanism for generating the former two distinct pools, metabolic origin of the mitochondrial malonyl-CoA pool is still unclear. In this study we demonstrate that malonyl-CoA synthetase encoded by the Arabidopsis AAE13 (AT3G16170) gene is dual-localized, in the cytosol and mitochondria. These proteins are translated from two types of transcripts, one that encompasses and one that does not encompass a mitochondrial targeting presequence. Whereas the cytosolically localized AAE13 protein is probably not essential due to the presence of a redundant malonyl-CoA generating system provided by a cytosolic acetyl-CoA carboxylase, the mitochondrially localized AAE13 protein is essential for plant growth. Phenotypes of aae13-1 mutant are transgenically reversed only if the mitochondrial presequence is present in the ectopically expressed AAE13 proteins. The aae13- 1 mutant exhibits typical metabolic phenotypes associated with a deficiency in the mitochondrial fatty acid synthase system, namely depleted lipoylation of the H subunit of the photorespiratory enzyme glycine decarboxylase, increased accumulation of glycine and glycolate, and reduced levels of sucrose. Most of these metabolic alterations, and associated morphological changes, are reversed when the aae13-1 mutant is grown in a non-photorespiratory condition (i.e. 1% CO2 atmosphere), demonstrating that they are a consequence of the deficiency in photorespiration due to the inability to generate lipoic acid from mitochondrially synthesized fatty acids.

Keywords

malonyl-CoA synthetase, mitochondrial fatty acid synthase, lipoic acid, glycine decarboxylase, photorespiration, and Arabidopsis thaliana

Disciplines

Biochemistry, Biophysics, and Structural Biology | Genetics and Genomics | Molecular Biology | Plant Sciences

Comments

This is the peer reviewed version of the following article: Guan, Xin, and Basil J. Nikolau. "AAE 13 encodes a dual-localized malonyl-CoA synthetase that is crucial for mitochondrial fatty acid biosynthesis." *The Plant Journal* 85, no. 5 (2016): 581-593., which has been published in final form at doi:10.1111/tpj.13130. This article may be used for non-commercial purposes in accordance with Wiley Terms and Conditions for Use of Self-Archived Versions. This article may not be enhanced, enriched or otherwise transformed into a derivative work, without express permission from Wiley or by statutory rights under applicable legislation. Copyright notices must not be removed, obscured or modified. The article must be linked to Wiley's version of record on Wiley Online Library and any embedding, framing or otherwise making available the article or pages thereof by third parties from platforms, services and websites other than Wiley Online Library must be prohibited.

This article is available at Iowa State University Digital Repository: https://lib.dr.iastate.edu/bbmb_ag_pubs/322

Received Date : 25-Nov-2015
Revised Date : 12-Jan-2016
Accepted Date : 18-Jan-2016
Article type : Original Article

Author Manuscript

Running title: Arabidopsis mitochondrial fatty acid synthase

AAE13 encodes a dual-localized malonyl-CoA synthetase that is crucial for mitochondrial fatty acid biosynthesis

Xin Guan[1,2], and Basil J. Nikolau[1,2,3,*]

[1]*Department of Biochemistry, Biophysics, and Molecular Biology, Iowa State University, Ames, Iowa 50011*

[2]*The NSF Engineering Research Center for Biorenewable Chemicals (CBiRC), Iowa State University, Ames, Iowa 50011*

[3]*Center for Metabolic Biology, Iowa State University, Ames, Iowa 50011*

***For correspondence** (Basil J. Nikolau; email, dimmas@iastate.edu; tel, 515-294-9423; and fax, 515-294-0453)

Email addresses: Xin Guan, xguan@iastate.edu; and Basil J. Nikolau, dimmas@iastate.edu.

Key words: malonyl-CoA synthetase, mitochondrial fatty acid synthase, lipoic acid, glycine decarboxylase, photorespiration, and Arabidopsis thaliana

Total word count (significance statement, summary, introduction, results, discussion, experimental procedures, and acknowledgements): 5970

This is the author manuscript accepted for publication and has undergone full peer review but has not been through the copyediting, typesetting, pagination and proofreading process, which may lead to differences between this version and the Version of Record. Please cite this article as doi: 10.1111/tpj.13130

This article is protected by copyright. All rights reserved

Breakdown of the word count: significance statement, 48; summary, 251; introduction, 633; results, 2768; discussion, 1761; experimental procedures, 825; acknowledgements, 135; references, 2142; figure legends, 562; and supporting figure/table/method legends, 535.

Author Manuscript

SUMMARY

Malonyl-CoA is a key intermediate in a number of metabolic processes associated with its role as a substrate in acylation and condensation reactions. These types of reactions occur in plastids, the cytosol and mitochondria, and although carboxylation of acetyl-CoA is the known mechanism for generating the former two distinct pools, metabolic origin of the mitochondrial malonyl-CoA pool is still unclear. In this study we demonstrate that malonyl-CoA synthetase encoded by the Arabidopsis *AAE13* (AT3G16170) gene is dual-localized, in the cytosol and mitochondria. These proteins are translated from two types of transcripts, one that encompasses and one that does not encompass a mitochondrial targeting presequence. Whereas the cytosolically localized AAE13 protein is probably not essential due to the presence of a redundant malonyl-CoA generating system provided by a cytosolic acetyl-CoA carboxylase, the mitochondrially localized AAE13 protein is essential for plant growth. Phenotypes of *aae13-1* mutant are transgenically reversed only if the mitochondrial presequence is present in the ectopically expressed AAE13 proteins. The *aae13-1* mutant exhibits typical metabolic phenotypes associated with a deficiency in the mitochondrial fatty acid synthase system, namely depleted lipoylation of the H subunit of the photorespiratory enzyme glycine decarboxylase, increased accumulation of glycine and glycolate, and reduced levels of sucrose. Most of these metabolic alterations, and associated morphological changes, are reversed when the *aae13-1* mutant is grown in a non-photorespiratory condition (i.e. 1% CO_2 atmosphere), demonstrating that they are a consequence of the deficiency in photorespiration due to the inability to generate lipoic acid from mitochondrially synthesized fatty acids.

This article is protected by copyright. All rights reserved

INTRODUCTION

Acyl carboxylates are activated in metabolic processes by their acylation via a thioester bond to Coenzyme A (CoA). The resulting energy-rich acyl-CoAs are intermediates of metabolism that are used to assemble or are products of disassembly of a variety of different metabolites (e.g. fatty acids and amino acids). The importance of these intermediates in plant metabolism maybe reflected in the large number of acyl-CoA synthetases that are found in plant genomes; for example Arabidopsis contains 44 genes that are recognizable by sequence comparison as acyl-CoA synthetases (Shockey et al., 2003). Malonyl-CoA is one such important metabolic intermediate, which participates in two types of metabolic processes: a) as the acyl-donor in acylation of hydroxyl-groups or amine-groups to form malonylated esters (Suzuki et al., 2002; Taguchi et al., 2005) or amides (Guo et al., 1993); and b) as the 2-carbon donor substrate in the extension reactions of polyketide (Stewart et al., 2013) and fatty acid (Li-Beisson et al., 2013; Ohlrogge and Browse, 1995) biosynthesis.

Metabolic processes that require malonyl-CoA as a substrate are known to occur in plastids, the cytosol and mitochondria. In plastids and the cytosol malonyl-CoA is generated via the ATP-dependent carboxylation of acetyl-CoA, which is catalyzed by isozymes of acetyl-CoA carboxylase (ACCase) (Nikolau et al., 2003). The cytosolic malonyl-CoA pool is used in the assembly of polyketides, as exemplified by the chalcone synthase-catalyzed reaction (Austin and Noel, 2003), and in the elongation of preexisting fatty acids by an ER-localized fatty acid elongase (FAE) (James et al., 1995). In plastids, the malonyl group of malonyl-CoA is first transacylated to the phosphopantetheine cofactor of acyl carrier protein (ACP) and used as the substrate of the plastidial fatty acid synthase (ptFAS) system that generates fatty acids *de novo* with acetyl-CoA as the other substrate (Li-Beisson et al., 2013).

This article is protected by copyright. All rights reserved

Author Manuscript

Mitochondria also require malonyl-CoA to support the biosynthesis of fatty acids, and these fatty acids are primarily destined for the biosynthesis of lipoic acid (Li-Beisson et al., 2013; Wada et al., 1997). The metabolic source of the mitochondrial malonyl-CoA is unclear in plant cells. Although a mitochondria-located ACCase has been reported in Poaceae (i.e. barley (Focke et al., 2003) and rice (Heazlewood et al., 2003)), this has not been validated by the genomics-based evidence. Animal cells and yeast import malonate into mitochondria via a carnitine shuttle (Bieber, 1988). The role of carnitine in plant metabolism is not so clear. A gene potentially encoding an acyl carnitine carrier-like enzyme has been identified in plants (Lawand et al., 2002), but mutation in this gene does not show a phenotype typical of deficiency in mitochondrial fatty acid synthase (mtFAS) system (Eisenhut et al., 2013). Furthermore, carnitine levels in plant tissues are between 1/100th and 1/1000th of the levels found in animal cells (Bourdin et al., 2007), making this an unlikely mechanism.

In addition to the ACCase-catalyzed mechanism for generating malonyl-CoA, a malonyl-CoA synthetase (encoded by *MatB* of bacteria (An and Kim, 1998; Koo and Kim, 2000), *AAE13* (AT3G16170) of Arabidopsis (Chen et al., 2011; Wang et al., 2014), and *ACSF3* of humans (Witkowski et al., 2011)) has been characterized, providing an alternative route for generating malonyl-CoA from free malonate. Prior characterizations have indicated that the Arabidopsis *AAE13*-encoded malonyl-CoA synthetase is cytosolically localized, serving as an alternative source of cytosolic malonyl-CoA (Chen et al., 2011). In this study we characterized the 5' leader sequence of the *AAE13* gene and identified that it encodes a dual-targeted protein, located in both the cytosol and mitochondria. Biochemical and morphological characterizations of the *aae13-1* mutant indicate that the cytosolic malonyl-CoA synthetase function is not limiting to plant metabolism and development, probably because the cytosolically located ACCase can also generate malonyl-CoA. More significantly, mitochondrial malonyl-CoA synthetase function is crucial to plant metabolism and development, confirming a role of the *AAE13* gene in supporting the mtFAS system.

This article is protected by copyright. All rights reserved

Author Manuscript

RESULTS

Cloning of 5 *AAE13* transcript variants

5' RACE analysis of the *AAE13* transcript identified multiple variants, which differ in the length of the 5'-UTR (Figure 1a). Cloning and sequencing of these 5'-RACE products identified 5 transcript variants (*AAE13.1* to *AAE13.5*), which appear to be products of alternative transcriptional initiation (Figure 1b; and Figure S1 for details). All these variants span the first intron of the *AAE13* gene, however the resultant transcripts could initiate protein translation from alternative "ATG" codons; these we label as the Exon1 "ATG" and Exon2 "ATG", indicating their positions in exon 1 and 2, respectively. Transcripts *AAE13.1* and *AAE13.2* would initiate translation from Exon1 "ATG", which resides in the context of a typical Kozak sequence (adenosine at position -3, and guanine at position +4 (Kozak, 1986)) for efficient translation initiation. Translation from this "ATG" codon would generate a protein of 608 amino acids. In contrast, transcript variants *AAE13.3*, *AAE13.4* and *AAE13.5*, are shorter at the 5' end and lack Exon1 "ATG". These transcripts would be predicted to initiate protein translation from Exon2 "ATG", but its context (cytosine at position -3, and guanine at position +4) does not match the eukaryotic Kozak sequence (Kozak, 1986). Translation from this latter "ATG" start codon would generate a protein that is 64 residues shorter than the protein encoded by *AAE13.1* and *AAE13.2*.

Based on the cloning recovery rates of each variant, from a pool of 80 clones that were analyzed, the relative abundance of these 5 variants is 5%, 20%, 30%, 30%, and 15%, respectively (Figure 1b). These data indicate that the transcripts that do not contain Exon1 "ATG" (*AAE13.3*, *AAE13.4* and *AAE13.5*) are 3-fold more abundant than the transcripts that contain Exon1 "ATG" (*AAE13.1* and *AAE13.2*). Additional confirmation of this ratio was obtained from previously published RNA-Seq data (Bonawitz et al., 2014). Short reads of the wild-type plants were mapped (*e*-value < 10e-12) to the 5' end of the *AAE13* transcript variants (Figure S2). These data also indicate that transcripts that lack Exon1

This article is protected by copyright. All rights reserved

Author Manuscript

"ATG" are more abundant than transcripts that contain Exon1 "ATG"; in this case by a factor of 4-fold.

This 64-residue sequence that is encoded by *AAE13.1* and *AAE13.2*, but is absent from the other 3 transcripts, lacks acidic amino acids but is rich in basic residues, these being features that are characteristic of mitochondrial targeting presequence elements. Indeed, analysis with MitoProt II (36 N-terminal residues with a score of 0.9841) (Claros and Vincens, 1996) and PSORT (with a score of 0.581) (Nakai and Horton, 1999) predict that it is a mitochondrial targeting presequence.

We also conducted *in silico* analyses of the 5' coding sequences (CDS) of *AAE13* orthologs in other 8 plant species, whose genomes have been sequenced and are publically available at PlantGDB (www.plantgdb.org (Duvick et al., 2008)) (Figure S3). All plant species tested contain 5' leader sequences, all of which encode amino acid sequences that are predicted to be a mitochondrial targeting presequence.

The 5' leader sequence of *AAE13* encodes a mitochondrial presequence

The AAE13 protein encoded by *AAE13.3*, *AAE13.4* and *AAE13.5* transcripts encoding proteins whose translation initiates at the Exon2 "ATG" start codon, has been demonstrated to be cytosolic (Chen et al., 2011). Transgenic experiments were performed with a GFP-tagged fusion protein to evaluate the computational prediction of the organelle targeting capability of the newly identified N-terminal leader sequence of the AAE13 protein that is encoded by transcripts *AAE13.1 and AAE13.2*. These experiments tested the ability of the N-terminal 86 residues encoded by the 5' 258 bp of *AAE13.1* or *AAE13.2* to direct the subcellular localization of GFP. This 86-residue sequence is encoded by both exon 1 and 2, and contains both putative Exon1 and Exon2 "ATG" start codons.

Figure 2 shows confocal micrographs of roots and leaf mesophyll cells of the resulting transgenic plants. MitoTracker Orange was used on roots as a mitochondrial marker, and chlorophyll autofluorescence was simultaneously

This article is protected by copyright. All rights reserved

Author Manuscript

recorded in leaves as a chloroplastic marker. In roots the GFP fluorescence obtained from the P_{35S}*::AAE13*$_{258}$*-GFP* transgene overlaps with the MitoTracker Orange signal, indicating a mitochondrial localization of the GFP-fusion protein. Similar discrete subcellular GFP signals were observed in leaves that are distinct from the chlorophyll autofluorescence, revealing that the GFP-fusion protein is not localized to chloroplast, and are consistent with a mitochondrial location. The negative control plants that carry a P_{35S}*::GFP* transgene exhibit GFP fluorescence in the cytosol and nuclei of roots and leaves as previously reported (Guan et al., 2015), and the non-transgenic wild-type control plants do not exhibit any fluorescence that matches to the GFP wavelength in either roots or leaves. We therefore conclude that the N-terminal 86-residue sequence of the protein encoded by *AAE13.1* and *AAE13.2* is a mitochondrial targeting presequence.

Expression of the *AAE13* gene in different Arabidopsis organs

The spatial and temporal expression pattern of the *AAE13* gene was determined using quantitative RT-PCR with RNA preparations extracted from different organs, using primers that determine the integrated levels of all five transcriptional variants or with primers that determine the levels of only the variants that encode the mitochondrially localized protein (i.e. *AAE13.1* and *AAE13.2*). The two sets of primers produce parallel expression data (Figure 3). The expression of *AAE13* gene occurs in all organs tested, with an approximately 3-fold difference between the highest (i.e. flower) and lowest (i.e. roots and rosette leaves) expression levels. This near ubiquitous expression pattern of the *AAE13* gene is consistent with the microarray data visualized by the Arabidopsis eFP Browser (Schmid et al., 2005; Winter et al., 2007), and is also comparable with the expression pattern of other already characterized mtFAS components, such as the *mtPPT* gene (Guan et al., 2015).

Genetic complementation of the *aae13-1* mutant

Our discovery that the *AAE13* gene can express transcripts that either contain (*AAE13.1* and *AAE13.2*) or lack (*AAE13.3*, *AAE13.4* and *AAE13.5*) a sequence

This article is protected by copyright. All rights reserved

Author Manuscript

coding for an N-terminal mitochondrial targeting presequence indicates that this gene encodes a malonyl-CoA synthetase that is dual-localized to mitochondria (designated as the mtAAE13 protein) and the cytosol (designated as the ctAAE13 protein). Therefore, dissecting the function of this gene is more complex and needs strategic experimentation to decipher the characterization of *aae13-1* mutant (Chen et al., 2011).

The T-DNA-tagged *aae13-1* mutant line expresses an extreme growth phenotype (Chen et al., 2011), and in our experimental conditions at 16 day-after-imbibition (DAI), the growth of this mutant is arrested at between the stages 1.00 and 1.02, based on the classification system that was previously describe (Boyes et al., 2001) (i.e. exhibiting cotyledons and two emerged rosette leaves of about 1 mm in length), whereas the wild-type plants develop to the stage 1.06 (i.e. exhibiting six rosette leaves that are longer than 1 mm in length) (Figure 5). We designed a genetic complementation experiment to distinguish whether the phenotype associated with the *aae13-1* mutant is due to the loss of one or the other AAE13 functions that are expressed in the two subcellular compartments. Specifically, the *aae13-1* mutant plants were transformed with three different versions of 35S promoter-driven *AAE13* transgenes. One of these carried the wild-type *AAE13.1* CDS (*mtAAE13*), which encodes both Exon1 and Exon2 "ATG" codons (P_{35S}::$mtAAE13_{ATG\text{-}ATG}$). The two other constructs carried mutated *mtAAE13* transgenes in which either the Exon2 or Exon1 "ATG" codons were replaced by a "CTG" codon (i.e. P_{35S}::$mtAAE13_{ATG\text{-}CTG}$ and P_{35S}::$mtAAE13_{CTG\text{-}ATG}$, respectively) (Figure 4a). The former point mutation eliminates the Exon2 "ATG" codon to avoid any residual protein translation at this start codon that generates the ctAAE13 protein, whereas the latter point mutation eliminates the Exon1 "ATG" codon and eliminates the translation of the mtAAE13 protein. Twenty to thirty independent transformants were recovered for each of these transformations, and two independent lines for each transgene were selected for characterization.

This article is protected by copyright. All rights reserved

Author Manuscript

The T-DNA-tagged *aae13-1* mutant lines carrying the P_{35S}*::mtAAE13*$_{ATG-ATG}$ and P_{35S}*::mtAAE13*$_{ATG-CTG}$ transgenes reverse the growth deficiency associated with the *aae13-1* mutation, and the morphology of these plants is near wild-type (Figure 4b). In comparison, the plants carrying the transgene that lacks the Exon1 "ATG" codon (i.e. P_{35S}*::mtAAE13*$_{CTG-ATG}$) fails to rescue the *aae13-1* growth phenotype (Figure 4b). Namely, the phenotype of these transgenic plants is near identical to the *aae13-1* mutant transformed with an empty plasmid (Figure 4b).

These results demonstrate that the expression of the mtAAE13 protein, but not the ctAAE13 protein, is capable of complementing the loss of *AAE13* gene functions. These findings are in complete agreement and clarify the previous observations that the 35S promoter-driven *ctAAE13* (P_{35S}*::ctAAE13*) fails to rescue the *aae13-1* phenotype, whereas the expression of the *ctAAE13* under control of its native promoter (P_{AAE13}*::AAE13*) can rescue this phenotype (Chen et al., 2011). The difference is due to the fact that the latter transgene, which encompasses the *AAE13* "promoter element" also contains the genetic elements that are needed to generate all 5 *AAE13* transcript variants, including those (*AAE13.1* and *AAE13.2*) that encode the mtAAE13 protein.

Chemical complementation of the *aae13-1* mutant

Realizing the crucial nature of *AAE13* gene function as encoding a mitochondrial protein we considered that it could generate the mitochondrial malonyl-CoA that is used as the substrate for the mitochondrial fatty acid biosynthesis. Because prior characterizations of mutants that affect the normal operation of the mtFAS system present a growth deficiency, which is rescueable by growing plants in an elevated CO_2 atmosphere (Ewald et al., 2007; Guan et al., 2015), we tested if the *aae13-1* mutant phenotype could be similarly rescued. This was accomplished by growing the *aae13-1* mutant and wild-type plants in ambient air and in an atmosphere enriched with 1% CO_2. As already described at 16 DAI in the ambient air atmosphere, growth of the *aae13-1* mutant is arrested at between the stages 1.00 and 1.02, in contrast when these plants are grown in the 1% CO_2

This article is protected by copyright. All rights reserved

Author Manuscript

atmosphere, the *aae13-1* mutant grows vigorously to the stage 1.06 (i.e. exhibiting six rosette leaves), nearing a wild-type appearance (Figure 5). This reversal of the growth phenotype in the 1% CO_2 atmosphere is a trait typical of deficiency in photorespiration (Somerville and Ogren, 1979), as synthesis of 2-phosphoglycolate by ribulose-1,5-bisphosphate carboxylase/oxygenase is inhibited in the 1% CO_2 atmosphere.

Alterations in the protein lipoylation status in the *aae13-1* mutant

Because mtFAS generates the precursor for lipoic acid biosynthesis, we further tested the hypothesized role of the *AAE13* gene in generating the malonyl-CoA substrate for mtFAS, by assaying the lipoylation status of the known lipoylated proteins in the *aae13-1* mutant plants. These assays were conducted via western blot analysis with anti-lipoic acid antibodies. All plants for these analyses were grown in the 1% CO_2 atmosphere, to eliminate the bias associated with the morphological deficiency of the *aae13-1* mutant. SDS-PAGE analysis of protein extracted from *aae13-1* and the control plants do not indicate any dramatic difference in the proteomes of these plants (Figure 6a), but western blot assays with anti-lipoic acid antibodies indicate that the most dramatic alteration is the complete elimination of the lipoic acid cofactor of H protein subunit of glycine decarboxylase complex (GDC) (Figure 6b). Parallel analysis with anti-H protein antibodies indicates that this effect is due to under-lipoylation of the H protein, because the level of the H protein itself is unchanged in the *aae13-1* mutant (Figure 6b).

Figure 6b also reveals the lipoylation status of three additional lipoylated proteins, two that occur in mitochondria (i.e. E2 subunits of mitochondrial pyruvate dehydrogenase (PDH) and α-ketoglutarate dehydrogenase (KGDH)), and one that occurs in plastids (i.e. E2 subunit of plastidial PDH) (Guan et al., 2015). While lipoylation of the E2 subunit of plastidial PDH was unaffected, lipoylation of all three mitochondrial proteins are reduced in the *aae13-1* mutant, to levels between 20% and 50% of the wild-type control plants. In all cases, the lipoylation status of these mitochondrial proteins return to the wild-type levels in

This article is protected by copyright. All rights reserved

Author Manuscript

the *aae13-1* mutant plants transgenic with the P_{AAE13}*::AAE13* transgene (Figure 6b), indicating that these are effects due to the lack of the *AAE13*-associated functions. These results therefore confirm the role of *AAE13* in the mtFAS system, contributing the malonyl-CoA building block for the biosynthesis of mitochondrial octanoyl-ACP, and the downstream lipoic acid that is restricted in the *aae13-1* mutant for the lipoylation of mitochondrial proteins.

Alterations in malonate metabolism in the *aae13-1* mutant

As would be expected by the deficiency in the *AAE13* function, the levels of the substrate for this gene product (i.e. malonate) is elevated in the *aae13-1* mutant to approximately 1.54 ± 0.10 µmol/g fresh tissue (0.24% of dry weight) in the aerial organs of the mutant plants, whereas in the wild-type plants malonate concentration is approximately 0.19 ± 0.05 µmol/g fresh tissue (0.03% of dry weight), being about 1/8th of the levels found in the mutant (Figure 7). However, in the transgenically complemented mutant plants (carrying the P_{AAE13}*::AAE13*, P_{35S}*::mtAAE13*$_{ATG\text{-}ATG}$, or P_{35S}*::mtAAE13*$_{ATG\text{-}CTG}$ transgenes) the accumulation of malonate is near wild-type levels (below 0.3 µmol/g fresh tissue) (Figure S4). Moreover, whereas growing the *aae13-1* mutant plants in a 1% CO_2 atmosphere reverses the growth phenotype of the mutant, malonate levels remain elevated at a concentration of 1.60 ± 0.04 µmol/g fresh weight of leaf tissue, 10-fold higher than the wild-type plants (Figure 7). Therefore, the increased accumulation of malonate is independent of the photorespiratory deficiency that is downstream of the mtFAS deficiency affected by the loss of the *AAE13* function.

We also evaluated the effect of feeding plants with malonate (Figure S5). In this experiment *aae13-1* mutant plants carrying P_{35S}*::R50*, P_{35S}*::mtAAE13*$_{ATG\text{-}ATG}$, P_{35S}*::AAE13*$_{ATG\text{-}CTG}$, or P_{35S}*::AAE13*$_{CTG\text{-}ATG}$ were grown in the absence or presence of 1 mM malonate in the 1% CO_2 atmosphere. The exogenously provided malonate appears to have been taken up by the plants as evidenced by the elevated levels of tissue malonate content in the aerial organs, to levels beyond those measured in the *aae13-1* mutant plants (Figure 7). Moreover, those plants that express a functional mtAAE13 protein (i.e. plants carrying

This article is protected by copyright. All rights reserved

Author Manuscript

P_{35S}::*AAE13*$_{ATG-ATG}$ or P_{35S}::*AAE13*$_{ATG-CTG}$) are larger than those that lack this function (i.e. plants carrying P_{35S}::*R50* or P_{35S}::*AAE13*$_{CTG-ATG}$). We interpret these findings that the toxic effect of malonate is located to mitochondria, as the presence of a functional mtAAE13 protein would metabolize the malonate to malonyl-CoA and beyond to lipoic acid, thus reduce its toxic effect.

Metabolic alterations in the *aae13-1* mutant

Because *AAE13* appears to have a role in mitochondrial fatty acid biosynthesis, and the associated supply of the lipoic acid cofactor for GDC to metabolize photorespiratory glycine, we also performed metabolic analyses, which were primarily focused on fatty acids, amino acids, glycolate, and sucrose. Plants used in these analyses were grown either in an ambient atmosphere where the alterations associated with photorespiratory deficiency are present, or in the 1% CO_2 atmosphere where the alterations associated with photorespiratory deficiency are suppressed (Figure 7).

In ambient air the *aae13-1* mutant displays a markedly reduced accumulation of most fatty acids, these being as low as 10% of the wild-type levels (e.g. 16:3). The fatty acid 16:3 is almost exclusively found in plastidial galactolipids (Li-Beisson et al., 2013), therefore its depletion may indicate the reduction in the thylakoid membrane system. The most dramatic metabolic alteration is the 250-fold hyperaccumulation of glycine in the *aae13-1* mutant. This is readily explainable as a consequence of the depleted lipoylation of GDC, which blocks the ability to metabolize photorespiratory glycine (Ewald et al., 2007; Guan et al., 2015). Consistent with this block in the metabolism of photorespiratory intermediates is a 4-fold increase in glycolate levels, the precursor of photorespiratory glycine. In addition, with the inability to recover photorespiratory carbon, sucrose levels (i.e. the transported form of sugar) are reduced to below 2% of the control levels. Finally, as an indicator of the close interrelationship between carbon and nitrogen metabolism, several amino acids, other than glycine, exhibit increased accumulation (e.g. glutamine, lysine, and leucine); the

This article is protected by copyright. All rights reserved

Author Manuscript

one most affected is alanine, whose concentration is increased by up to 21-fold of the control level.

Growing the *aae13-1* mutant plants in the 1% CO_2 atmosphere restored the accumulation of most of these metabolites to near the wild-type level (Figure 7), and similar restorations were observed in the transgenically rescued *aae13-1:*P_{AAE13}*::AAE13*, *aae13-1:*P_{35S}*::mtAAE13*$_{ATG-ATG}$, and *aae13-1:*P_{35S}*::mtAAE13*$_{ATG-CTG}$ plants grown in ambient air (Figure S4). The exceptions to the restoration by the 1% CO_2 treatment were the 3 amino acids, glycine, alanine, and glutamate (Figure 7). Although their levels did not return to wild-type levels, their concentrations are considerably reduced in the *aae13-1* mutant from the levels that occur in the ambient air atmosphere (only 30-, 3- and 2-fold above the wild-type levels). In combination these findings illustrate that these metabolic changes are directly a consequence of the missing mtAAE13 function, particularly associated with the photorespiratory deficiency as the consequence of the inability of the *aae13-1* mutant to produce the lipoic acid cofactor for GDC.

Author Manuscript

DISCUSSION

In plant cells malonyl-CoA serves as a substrate in two classes of metabolic reactions. One of these is the acylation of hydroxyl- or amine-groups to generate such specialized metabolites as malonylated anthocyanin and flavonoid glycosides (Suzuki et al., 2002; Taguchi et al., 2005), and N-malonylated derivative of the ethylene precursor, 1-aminocyclopropane-1-carboxylic acid (Guo et al., 1993). The other class of metabolic reactions that use malonyl-CoA, and the metabolically closely related malonyl-ACP, is the decarboxylative Claissen condensation reaction that is at the core of assembling complex polyketides (Stewart et al., 2013) and fatty acids (Li-Beisson et al., 2013). Both these latter biochemical processes are catalyzed by highly homologous enzymes that utilize malonyl-CoA/ACP as the 2-carbon donors in reactions that form 3-keto-acyl derivatives that are 2-carbons longer than the accepting substrate that

This article is protected by copyright. All rights reserved

is used in the condensation reaction (Li-Beisson et al., 2013; Stewart et al., 2013). The processes of polyketide biosynthesis (reactions catalyzed for example by chalcone synthase (Austin and Noel, 2003) or pyrone synthase (Jez et al., 2000)) are generally located in the cytosol of plant cells. However, there are three fatty acid forming systems in plant cells, located in plastids, mitochondria, and the ER membranes (Li-Beisson et al., 2013). The plastidial and mitochondrial systems are Type II FAS systems that use acyl-ACP intermediates. The ER-located FAE system utilizes preexisting acyl-CoA substrates and extends these to chain-lengths of 20 carbons and longer (James et al., 1995).

Characterization of ACCase isozymes that occur in plastids (Chen et al., 2009; Li et al., 2011; Reverdatto et al., 1999; Sun et al., 1997; Thelen and Ohlrogge, 2002a; Thelen and Ohlrogge, 2002b) and the cytosol (Baud et al., 2003; Lu et al., 2011; Yanai et al., 1995) has demonstrated that the plastidic and cytosolic pools of malonyl-CoA are each generated through the carboxylation of acetyl-CoA. These two separate pools of malonyl-CoA are metabolically distinct, as the plastidic envelope membranes are a physical barrier that does not allow the free movement of CoA derivatives (Brosnan et al., 1973; Fritz and Yue, 1963), and genetic evidence establishes that the two pools are not compensatory for the absence of one or the other (Baud et al., 2003; Li et al., 2011; Lu et al., 2011).

Hence one has to postulate that mitochondria are also equipped with its own enzymatic system for generating malonyl-CoA for mtFAS. Prior studies have suggested the role of a carnitine-like shuttle to import cytosolically generated malonyl-CoA (Lawand et al., 2002), as occurs in animal mitochondria (Bieber, 1988), or the possible involvement of a mitochondrially located ACCase (Focke et al., 2003; Heazlewood et al., 2003). Solving this puzzle has been hampered by the fact that genetic components associated with these suggested mitochondrial malonyl-CoA generating systems have not been identified.

Mitochondrial malonyl-CoA is generated from malonate

This article is protected by copyright. All rights reserved

Author Manuscript

This study unequivocally demonstrates that the malonyl-CoA synthetase enzyme, previously identified as encoded by the Arabidopsis *AAE13* gene (Chen et al., 2011), generates the mitochondrial malonyl-CoA pool by ligating malonate to CoA. This result is consistent with a previous finding that malonyl-CoA synthetase activity is measurable in the soluble fraction of purified pea mitochondria (Gueguen et al., 2000). Furthermore, this finding with the Arabidopsis AAE13 protein can be extrapolated generally among other higher plant species, because the N-terminal mitochondrial targeting leader presequence that occurs in the AAE13 protein also occurs in orthologs in higher plant species that have been sequenced (www.plantgdb.org (Duvick et al., 2008)). Thus, *in silico* predictions indicate that plant mitochondria in general can generate malonyl-CoA *in organello* from malonate. This reflects the situation that occurs in human mitochondria, where malonyl-CoA is similarly assembled from malonate via the reaction catalyzed by the ACSF3 protein, a malonyl-CoA synthetase (Witkowski et al., 2011). In contrast however, yeast mitochondria generate malonyl-CoA by the carboxylation of acetyl-CoA, catalyzed by a homomeric acetyl-CoA carboxylase isoform (Hfa1p) (Hoja et al., 2004). Similarly, mitochondrially located ACCase has been reported in Poaceae (i.e. barley (Focke et al., 2003) and rice (Heazlewood et al., 2003)) via proteomic analyses. However, additional genomic characterizations have not validated these mitochondrial ACCase findings.

The *AAE13* gene in fact expresses dual-localized proteins that we labeled as mtAAE13 and ctAAE13, and these appear to be translated from two classes of transcripts. CtAAE13 is encoded by three transcripts (*AAE13.3*, *AAE13.4* and *AAE13.5*) that are translated from Exon2 “ATG” codon, and generates the malonyl-CoA synthetase activity that has been characterized in the cytosol (Chen et al., 2011). MtAAE13 is encoded by two transcripts (*AAE13.1* and *AAE13.2*) that are translated from the Exon1 “ATG” codon, and generates mitochondrially targeted malonyl-CoA synthetase activity. The ability of exogenous malonate to complement the loss of the cytosolic malonyl-CoA pool in ATP citrate lyase mutants is evidence in support of the cytosolically located malonyl-CoA

This article is protected by copyright. All rights reserved

Author Manuscript

synthetase (Fatland et al., 2005). However, ectopic expression of mtAAE13, and not ctAAE13, is required to reverse the alterations in morphology and metabolic homeostasis of the *aae13-1* mutant. Therefore, it is the loss of the ability to generate the mitochondrial malonyl-CoA pool, and not the cytosolic malonyl-CoA pool that generates the *aae13-1* mutant phenotypes.

The findings presented herein now lead to the question of the metabolic origin of malonate. Although malonate can occur at relatively high levels in plant systems, particularly in roots and nodules of legumes, accounting for as much as 4% of the dry weight of these tissues (Li and Copeland, 2000), in the aerial organs of Arabidopsis we have measured a relatively lower malonate content, accounting 0.03% of dry weight. As would be expected this level is elevated by about 8-fold in the *aae13-1* mutant. Several hypotheses have been proposed concerning the potential metabolic sources of malonate. Given the mitochondrial location of the mtAAE13 protein, malonate could be generated from a metabolic pathway that occurs within mitochondria, for example the decarboxylation of oxaloacetate (de Vellis et al., 1963; Shannon et al., 1963). Alternatively, it is possible that free malonate is generated in the cytosol by the hydrolysis of malonyl-CoA (Stumpf and Burris, 1981), and is subsequently taken up by mitochondria (Wada et al., 1997). However, this would be a highly energy-expensive route, and as pointed out earlier the only known malonate translocator is carnitine-dependent, which is expressed at low levels (Bourdin et al., 2007). Another possible source of malonate is from the oxidation of malondialdehyde, a toxic metabolite that is derived from peroxidation of polyunsaturated fatty acids (Chen et al., 2011).

AAE13 contributes to mtFAS and photorespiration

The physiological role of the *AAE13* gene product in generating the malonyl-CoA substrate of the mtFAS system is implicated by the phenotypic and biochemical characterizations of the *aae13-1* mutant. Consistent with the major role of mtFAS in synthesizing the octanoyl-ACP precursor that is used for mitochondrial lipoic acid biosynthesis (Wada et al., 2001a; Yasuno and Wada, 1998), the *aae13-1* mutant displays a photorespiratory phenotype associated with depletion of GDC

This article is protected by copyright. All rights reserved

Author Manuscript

lipoylation; GDC being one of the essential enzymes needed in metabolizing photorespiratory glycine (Bauwe et al., 2010). The phenotypic alterations that are exhibited by the *aae13-1* mutant include miniaturized aerial organs, hyperaccumulation of glycine, and alterations in many other metabolites associated with a block in photorespiration (i.e. fatty acids, amino acids, glycolate, and sucrose). These metabolic aberrations are reversed when the *aae13-1* mutant plants are grown in a non-photorespiratory condition (i.e. 1% CO_2 atmosphere). In addition, these phenotypic traits parallel those observed in other known mtFAS mutants (e.g. *mtkas* (Ewald et al., 2007) and *mtppt-rnai* (Guan et al., 2015) mutants), substantiating the essential role of *AAE13* in the mtFAS system.

The lipoylation states of other lipoylated proteins are either unaffected (i.e. plastidial PDH) or partially reduced (i.e. mitochondrial PDH and KGDH) in the *aae13-1* mutant. These results are consistent with the fact that plastids have their own enzymatic system to synthesize lipoic acid using plastidial octanoyl-ACP as the substrate (Wada et al., 2001b; Yasuno and Wada, 2002), therefore lipoylation of plastidial PDH is independent of the mtFAS system. In comparison, the partially reduced lipoylation of the mitochondrial PDH and KGDH may be due to the import of lipoic acid or substrates of lipoic acid biosynthesis (i.e. octanoate or octanoyl-CoA) downstream of the *AAE13* `function (Ewald et al., 2014).

AAE13 **may contribute to malonate detoxification**

Although growing the *aae13-1* mutant in the 1% CO_2 atmosphere considerably reverses the defective morphological appearance of these plants, they do not completely recover to a wild-type state. This contrasts with other strains that are blocked in the mtFAS function (e.g. *mtkas* (Ewald et al., 2007) and *mtppt-rnai* (Guan et al., 2015) mutants), and in mutants that are deficient in photorespiration (e.g. *shmt* (Voll et al., 2006), *hpr* (Timm et al., 2008), and *bou* (Eisenhut et al., 2013) mutants). In both mtFAS and photorespiration mutants, growth in the elevated CO_2 atmosphere completely reverses the aberrant growth morphology that these plants present in ambient air. These findings indicate that the lack of

This article is protected by copyright. All rights reserved

Author Manuscript

malonyl-CoA synthetase function, in addition to affecting mtFAS-dependent photorespiration deficiency (that is reversible in the 1% CO_2 atmosphere), disturbs additional processes that are not reversible by growing the *aae13-1* mutant in the 1% CO_2 atmosphere. Because the ectopically expressed *mtAAE13* transgene completely reverses all the morphological and metabolic changes that are exhibited by the *aae13-1* mutant in ambient air, lack of this photorespiration-independent function is a consequence of the deficiency in the *mtAAE13* function, and not a consequence of the deficiency in the *ctAAE13* function that would result from the translation of *AAE13.3*, *AAE13.4* and *AAE13.5*, which lack the mitochondrial targeting presequence. This *ctAAE13* function is redundant to that provided by the cytosolically located homomeric ACCase (Baud et al., 2003; Lu et al., 2011; Yanai et al., 1995).

This photorespiration-independent phenotype that is maintained even when the *aae13-1* mutant is grown in the 1% CO_2 atmosphere maybe associated with the increased accumulation of malonate within mitochondria, but not in the other subcellular compartments. Indeed the malonate feeding experiments support this conclusion that plants that do not express a functional mtAAE13 grow smaller than those that could metabolize the mitochondrial malonate. Malonate is a competitive inhibitor of succinate dehydrogenase (Greene and Greenamyre, 1995; Quastel and Wooldridge, 1928), thus the increased accumulation of malonate within mitochondria due to the lack of mtAAE13 function could inhibit the TCA cycle. In addition, the TCA cycle could be further suppressed due to the reduced lipoylation states of mitochondrial PDH and KGDH that we characterized in the *aae13-1* mutant. While the results shown in this study do not formulate a firm explanation of the non-photorespiration basis of the morphological alteration in the *aae13-1* mutant, the prediction based on current knowledge suggests a role associated with malonate toxicity within mitochondria.

EXPERIMENTAL PROCEDURES

This article is protected by copyright. All rights reserved

Author Manuscript

Plant materials and genetic transformations

The Arabidopsis genetic stock carrying the *aae13-1* mutation (SALK_083785, Col-0 background) and the *aae13-1* mutant complemented by the P_{AAE13}::*AAE13* transgene were as previously mentioned (Chen et al., 2011). Confirmation of the T-DNA insertion in the *AAE13* gene was conducted with primers MS1-MS2 (genome specific) and MS3 (T-DNA specific; LBb1.3) (see Table S1 online for primer sequences).

For the GFP experiments, 5' CDS for 86 amino acid residues of *AAE13.1* was cloned with primers MS4-MS5, being designated as $AAE13_{258}$. For the genetic complementation experiment, full-length *AAE13.1* CDS was cloned with primers MS4-MS6, being designated as $mtAAE13_{ATG\text{-}ATG}$. Primers MS6-MS7 were used to generate a mutational *AAE13.1* CDS in which Exon1 "ATG" codon is replaced by "CTG", being designated as $mtAAE13_{CTG\text{-}ATG}$. A random DNA sequence of 50 bp was simulated using R (www.r-project.org) (see Method S1 online for the R code), and assembled using primers MS8-MS9, being designated as *R50*. All PCR products were cloned into pENTR/D-TOPO vector (Invitrogen, Carlsbad, CA), resulting in $AAE13_{258}$-ENTR, $mtAAE13_{ATG\text{-}ATG}$-ENTR, $mtAAE13_{CTG\text{-}ATG}$-ENTR, and *R50*-ENTR (see Table S2 online for the plasmid information). The Exon2 "ATG" in the $mtAAE13_{ATG\text{-}ATG}$-ENTR vector was replaced by "CTG" with primers MS10-MS11 using QuickChange II Site-Directed Mutagenesis Kit (Agilent Technologies, Santa Clara, CA), resulting in $mtAAE13_{ATG\text{-}CTG}$-ENTR. The genes in $AAE13_{258}$-ENTR was further sub-cloned into pEarleyGate103 (Earley et al., 2006), whereas genes in $mtAAE13_{ATG\text{-}ATG}$-ENTR, $mtAAE13_{ATG\text{-}CTG}$-ENTR, $mtAAE13_{CTG\text{-}ATG}$-ENTR and *R50*-ENTR were sub-cloned into pEarleyGate100 (Earley et al., 2006) using Gateway LR Clonase II Enzyme Mix (Invitrogen), respectively, resulting in the destination vectors $AAE13_{258}$-pEG103, $mtAAE13_{ATG\text{-}ATG}$-pEG100, $mtAAE13_{ATG\text{-}CTG}$-pEG100, $mtAAE13_{CTG\text{-}ATG}$-pEG100, and *R50*-pEG100. All destination vectors were used to transform Arabidopsis Col-0 wild-type plants (operated in ambient air) or the *aae13-1* homozygote

This article is protected by copyright. All rights reserved

Author Manuscript

(operated in the 1% CO_2 atmosphere) as previously described (Clough and Bent, 1998).

Seeds were sterilized and sown on Murashige and Skoog (MS) agar medium as describe previously (Jin et al., 2012). In the malonate feeding experiment the medium was supplemented with 1 mM malonate, and was adjusted to pH 5.7 before sterilization. After 4 days of stratification at 4 ℃ in the dark (initiated as 0 DAI), the plates were moved into growth chambers pumped with ambient air or 1% CO_2 for phenotypic analyses. The growth conditions were maintained at 22 ℃ under continuous illumination (photosynthetic photon flux density 100 μmol of photons m^{-2} s^{-1}).

Confocal microscopy

Confocal microscopy analysis was conducted on the wild-type control plants, the control transgenic plants carrying the P_{35S}*::GFP* transgene (Guan et al., 2015), and transgenic plants carrying the P_{35S}*::AAE13*$_{258}$*-GFP* transgene. Seedling plants at between 7 to 10 DAI were harvested for analysis as previously described (Guan et al., 2015). Specifically, roots were stained for 15min in the MS medium that contains 200 nM MitoTracker Orange (Invitrogen), and washed for 15min in the MS medium before analysis. Roots and mesophyll cells were examined using a Leica TCS NT confocal microscope system (Leica Microsystems). Laser wavelengths (excitation (nm) / emission (nm)) were applied as following: 489 / 500 to 535 for GFP, 543 / 560 to 600 for MitoTracker Orange, and 543 / 600 to 790 for chlorophyll autofluorescence.

5' RACE cloning

The 5' RACE analysis was performed with total RNA isolated from aerial organs of the wild-type plants at 16 DAI using SMARTer RACE cDNA Amplification Kit (Clontech Laboratories, Mountain View, CA). Following a round of PCR using primers MS12 (Short UPM), MS13 (Long UMP), and MS14 (*AAE13*-specific), nested PCR was performed using primers MS15 (NUP) and MS16 (*AAE13*-

Author Manuscript

This article is protected by copyright. All rights reserved

specific) following manufacturer's instruction. The PCR product was purified on a 2% agarose gel, and cloned into pCR4-TOPO vector (Invitrogen) for sequencing.

Quantitative RT-PCR

Quantitative RT-PCR was performed using the StepOnePlus Real-Time PCR System and SYBR Select Master Mix (Invitrogen) following manufacturer's instruction. *Actin-2* (AT3G18780) was used as the reference gene for relative quantification with primers MS17-MS18. Primers MS19-MS20 are specific for all 5 *AAE13* transcripts, whereas primers MS21-MS22 are specific for *AAE13.1* and *AAE13.2* transcripts.

Western blot

Total protein was extracted from 200 mg fresh aerial organs of plants at 16 DAI, which were grown in the 1% CO_2 atmosphere as described previously (Che et al., 2002). SDS-PAGE with 12.5% gel was applied to separate 50 mg total protein. Western blot analysis was performed with anti-lipoic acid antibodies (EMD Millipore, Billerica, MA) or with anti-H protein antibodies (a gift from Dr. David Oliver at Iowa State University) as described previously (Ewald et al., 2007; Guan et al., 2015).

Metabolic analyses

Plants were harvested at 16 DAI grown in a completely randomized design. Metabolite extracts (3 to 6 biological replicates) were prepared from aliquots of 50 mg fresh aerial organ tissue, and analyzed using multiple analytical platforms: Agilent 1200 HPLC system equipped with a fluorescence detector was used for amino acid analysis (Guan et al., 2015); and Agilent 7890 GC-MS system equipped with Agilent HP-5ms column was used for fatty acid (Lu et al., 2008), malonate, glycolate and sucrose (Duran et al., 2003) analyses. Log_2-ratio and SE were calculated as described previously (Quanbeck et al., 2012).

This article is protected by copyright. All rights reserved

Author Manuscript

ACKNOWLEDGEMENTS

The authors gratefully acknowledge Dr. John Browse (Washington State University, Pullman, WA) for the seed stocks of the *aae13-1* mutant line, and the *aae13-1* mutant transgenic line carrying the P_{AAE13}*::AAE13* transgene, and for valuable discussions of the manuscript. The WM Keck Metabolomics Research Laboratory and the Confocal Microscopy Facility (Iowa State University, Ames, IA) are acknowledged for providing access to instrumentation in the metabolic analyses and subcellular localization studies, respectively. The authors also acknowledge helpful discussions with Drs. Lloyd Sumner (The Samuel Roberts Noble Foundation, Ardmore, OK), Kazuki Saito (RIKEN Center for Sustainable Resource Science, Yokohama, Japan), Richard Dixon (University of North Texas, Denton, TX), and Libuse Brachova (Iowa State University, Ames, IA). This work was partially supported by grants from US National Science Foundation (Awards IOS1139489, EEC0813570 and MCB0820823) and the State of Iowa.

Author Manuscript

This article is protected by copyright. All rights reserved

SHORT LEGENDS FOR FIGURES AND SUPPLEMENTAL MATERIALS

Figure S1. Comparison of the nucleic acid sequences of the 5 *AAE13* transcript variants (the first 2 exons), and the *AAE13* genome sequence.

Figure S2. Short reads of RNA-Seq data mapped to the *AAE13* transcript variants.

Figure S3. *AAE13* orthologs in 9 plant species.

Figure S4. Metabolic alterations in the *aae13-1* mutant rescued by the genetic transgenes.

Figure S5. Malonate feeding of the *aae13-1* mutants.

Table S1. Nucleic acid sequences of DNA primers used in this study.

Table S2. Plasmids.

Method S1. R code used to simulate a random DNA sequence of 50 bp.

Author Manuscript

This article is protected by copyright. All rights reserved

REFERENCES

An, J.H., and Y.S. Kim. 1998. A gene cluster encoding malonyl-CoA decarboxylase (MatA), malonyl-CoA synthetase (MatB) and a putative dicarboxylate carrier protein (MatC) in Rhizobium trifolii--cloning, sequencing, and expression of the enzymes in Escherichia coli. *European journal of biochemistry / FEBS*. 257:395-402.

Austin, M.B., and J.P. Noel. 2003. The chalcone synthase superfamily of type III polyketide synthases. *Natural product reports*. 20:79-110.

Baud, S., V. Guyon, J. Kronenberger, S. Wuilleme, M. Miquel, M. Caboche, L. Lepiniec, and C. Rochat. 2003. Multifunctional acetyl-CoA carboxylase 1 is essential for very long chain fatty acid elongation and embryo development in Arabidopsis. *The Plant journal : for cell and molecular biology*. 33:75-86.

Bauwe, H., M. Hagemann, and A.R. Fernie. 2010. Photorespiration: players, partners and origin. *Trends in plant science*. 15:330-336.

Bieber, L.L. 1988. Carnitine. *Annual review of biochemistry*. 57:261-283.

Bonawitz, N.D., J.I. Kim, Y. Tobimatsu, P.N. Ciesielski, N.A. Anderson, E. Ximenes, J. Maeda, J. Ralph, B.S. Donohoe, M. Ladisch, and C. Chapple. 2014. Disruption of Mediator rescues the stunted growth of a lignin-deficient Arabidopsis mutant. *Nature*. 509:376-380.

Bourdin, B., H. Adenier, and Y. Perrin. 2007. Carnitine is associated with fatty acid metabolism in plants. *Plant physiology and biochemistry : PPB / Societe francaise de physiologie vegetale*. 45:926-931.

Boyes, D.C., A.M. Zayed, R. Ascenzi, A.J. McCaskill, N.E. Hoffman, K.R. Davis, and J. Gorlach. 2001. Growth stage-based phenotypic analysis of Arabidopsis: a model for high throughput functional genomics in plants. *The Plant cell*. 13:1499-1510.

Brosnan, J.T., B. Kopec, and I.B. Fritz. 1973. The localization of carnitine palmitoyltransferase on the inner membrane of bovine liver mitochondria. *The Journal of biological chemistry*. 248:4075-4082.

This article is protected by copyright. All rights reserved

Author Manuscript

Che, P., E.S. Wurtele, and B.J. Nikolau. 2002. Metabolic and environmental regulation of 3-methylcrotonyl-coenzyme A carboxylase expression in Arabidopsis. *Plant physiology*. 129:625-637.

Chen, H., H.U. Kim, H. Weng, and J. Browse. 2011. Malonyl-CoA synthetase, encoded by ACYL ACTIVATING ENZYME13, is essential for growth and development of Arabidopsis. *The Plant cell*. 23:2247-2262.

Chen, M., B.P. Mooney, M. Hajduch, T. Joshi, M. Zhou, D. Xu, and J.J. Thelen. 2009. System analysis of an Arabidopsis mutant altered in de novo fatty acid synthesis reveals diverse changes in seed composition and metabolism. *Plant physiology*. 150:27-41.

Claros, M.G., and P. Vincens. 1996. Computational method to predict mitochondrially imported proteins and their targeting sequences. *European journal of biochemistry / FEBS*. 241:779-786.

Clough, S.J., and A.F. Bent. 1998. Floral dip: a simplified method for Agrobacterium-mediated transformation of Arabidopsis thaliana. *The Plant journal : for cell and molecular biology*. 16:735-743.

de Vellis, J., L.M. Shannon, and J.Y. Lew. 1963. Malonic Acid Biosynthesis in Bush Bean Roots. I. Evidence for Oxaloacetate as Immediate Precursor. *Plant physiology*. 38:686-690.

Duran, A.L., J. Yang, L. Wang, and L.W. Sumner. 2003. Metabolomics spectral formatting, alignment and conversion tools (MSFACTs). *Bioinformatics*. 19:2283-2293.

Duvick, J., A. Fu, U. Muppirala, M. Sabharwal, M.D. Wilkerson, C.J. Lawrence, C. Lushbough, and V. Brendel. 2008. PlantGDB: a resource for comparative plant genomics. *Nucleic acids research*. 36:D959-965.

Earley, K.W., J.R. Haag, O. Pontes, K. Opper, T. Juehne, K. Song, and C.S. Pikaard. 2006. Gateway-compatible vectors for plant functional genomics and proteomics. *The Plant journal : for cell and molecular biology*. 45:616-629.

Eisenhut, M., S. Planchais, C. Cabassa, A. Guivarc'h, A.M. Justin, L. Taconnat, J.P. Renou, M. Linka, D. Gagneul, S. Timm, H. Bauwe, P. Carol, and A.P. Weber. 2013. Arabidopsis A BOUT DE SOUFFLE is a putative mitochondrial

This article is protected by copyright. All rights reserved

Author Manuscript

transporter involved in photorespiratory metabolism and is required for meristem growth at ambient CO(2) levels. *The Plant journal : for cell and molecular biology*. 73:836-849.

Ewald, R., C. Hoffmann, A. Florian, E. Neuhaus, A.R. Fernie, and H. Bauwe. 2014. Lipoate-Protein Ligase and Octanoyltransferase Are Essential for Protein Lipoylation in Mitochondria of Arabidopsis. *Plant physiology*. 165:978-990.

Ewald, R., U. Kolukisaoglu, U. Bauwe, S. Mikkat, and H. Bauwe. 2007. Mitochondrial protein lipoylation does not exclusively depend on the mtKAS pathway of de novo fatty acid synthesis in Arabidopsis. *Plant physiology*. 145:41-48.

Fatland, B.L., B.J. Nikolau, and E.S. Wurtele. 2005. Reverse genetic characterization of cytosolic acetyl-CoA generation by ATP-citrate lyase in Arabidopsis. *The Plant cell*. 17:182-203.

Focke, M., E. Gieringer, S. Schwan, L. Jansch, S. Binder, and H.P. Braun. 2003. Fatty acid biosynthesis in mitochondria of grasses: malonyl-coenzyme A is generated by a mitochondrial-localized acetyl-coenzyme A carboxylase. *Plant physiology*. 133:875-884.

Fritz, I.B., and K.T. Yue. 1963. Long-Chain Carnitine Acyltransferase and the Role of Acylcarnitine Derivatives in the Catalytic Increase of Fatty Acid Oxidation Induced by Carnitine. *Journal of lipid research*. 4:279-288.

Greene, J.G., and J.T. Greenamyre. 1995. Characterization of the excitotoxic potential of the reversible succinate dehydrogenase inhibitor malonate. *Journal of neurochemistry*. 64:430-436.

Guan, X., H. Chen, A. Abramson, H. Man, J. Wu, O. Yu, and B.J. Nikolau. 2015. A phosphopantetheinyl transferase that is essential for mitochondrial fatty acid biosynthesis. *The Plant journal : for cell and molecular biology*.

Gueguen, V., D. Macherel, M. Jaquinod, R. Douce, and J. Bourguignon. 2000. Fatty acid and lipoic acid biosynthesis in higher plant mitochondria. *The Journal of biological chemistry*. 275:5016-5025.

Guo, L., A.T. Phillips, and R.N. Arteca. 1993. Amino acid N-malonyltransferases from mung beans. Action on 1-aminocyclopropane-1-carboxylic acid and D-phenylalanine. *The Journal of biological chemistry*. 268:25389-25394.

This article is protected by copyright. All rights reserved

Author Manuscript

Heazlewood, J.L., K.A. Howell, J. Whelan, and A.H. Millar. 2003. Towards an analysis of the rice mitochondrial proteome. *Plant physiology*. 132:230-242.

Hoja, U., S. Marthol, J. Hofmann, S. Stegner, R. Schulz, S. Meier, E. Greiner, and E. Schweizer. 2004. HFA1 encoding an organelle-specific acetyl-CoA carboxylase controls mitochondrial fatty acid synthesis in Saccharomyces cerevisiae. *The Journal of biological chemistry*. 279:21779-21786.

James, D.W., Jr., E. Lim, J. Keller, I. Plooy, E. Ralston, and H.K. Dooner. 1995. Directed tagging of the Arabidopsis FATTY ACID ELONGATION1 (FAE1) gene with the maize transposon activator. *The Plant cell*. 7:309-319.

Jez, J.M., M.B. Austin, J. Ferrer, M.E. Bowman, J. Schroder, and J.P. Noel. 2000. Structural control of polyketide formation in plant-specific polyketide synthases. *Chemistry & biology*. 7:919-930.

Jin, H., Z. Song, and B.J. Nikolau. 2012. Reverse genetic characterization of two paralogous acetoacetyl CoA thiolase genes in Arabidopsis reveals their importance in plant growth and development. *The Plant journal : for cell and molecular biology*. 70:1015-1032.

Koo, H.M., and Y.S. Kim. 2000. Identification of active-site residues in Bradyrhizobium japonicum malonyl-coenzyme A synthetase. *Archives of biochemistry and biophysics*. 378:167-174.

Kozak, M. 1986. Point mutations define a sequence flanking the AUG initiator codon that modulates translation by eukaryotic ribosomes. *Cell*. 44:283-292.

Lawand, S., A.J. Dorne, D. Long, G. Coupland, R. Mache, and P. Carol. 2002. Arabidopsis A BOUT DE SOUFFLE, which is homologous with mammalian carnitine acyl carrier, is required for postembryonic growth in the light. *The Plant cell*. 14:2161-2173.

Li, J., and L. Copeland. 2000. Role of malonate in chickpeas. *Phytochemistry*. 54:585-589.

Li, X., H. Ilarslan, L. Brachova, H.R. Qian, L. Li, P. Che, E.S. Wurtele, and B.J. Nikolau. 2011. Reverse-genetic analysis of the two biotin-containing subunit genes of the heteromeric acetyl-coenzyme A carboxylase in Arabidopsis indicates a unidirectional functional redundancy. *Plant physiology*. 155:293-314.

This article is protected by copyright. All rights reserved

Author Manuscript

Li-Beisson, Y., B. Shorrosh, F. Beisson, M.X. Andersson, V. Arondel, P.D. Bates, S. Baud, D. Bird, A. Debono, T.P. Durrett, R.B. Franke, I.A. Graham, K. Katayama, A.A. Kelly, T. Larson, J.E. Markham, M. Miquel, I. Molina, I. Nishida, O. Rowland, L. Samuels, K.M. Schmid, H. Wada, R. Welti, C. Xu, R. Zallot, and J. Ohlrogge. 2013. Acyl-lipid metabolism. *The Arabidopsis book / American Society of Plant Biologists*. 11:e0161.

Lu, S., H. Zhao, E.P. Parsons, C. Xu, D.K. Kosma, X. Xu, D. Chao, G. Lohrey, D.K. Bangarusamy, G. Wang, R.A. Bressan, and M.A. Jenks. 2011. The glossyhead1 allele of ACC1 reveals a principal role for multidomain acetyl-coenzyme A carboxylase in the biosynthesis of cuticular waxes by Arabidopsis. *Plant physiology*. 157:1079-1092.

Lu, Y., L.J. Savage, I. Ajjawi, K.M. Imre, D.W. Yoder, C. Benning, D. Dellapenna, J.B. Ohlrogge, K.W. Osteryoung, A.P. Weber, C.G. Wilkerson, and R.L. Last. 2008. New connections across pathways and cellular processes: industrialized mutant screening reveals novel associations between diverse phenotypes in Arabidopsis. *Plant physiology*. 146:1482-1500.

Nakai, K., and P. Horton. 1999. PSORT: a program for detecting sorting signals in proteins and predicting their subcellular localization. *Trends in biochemical sciences*. 24:34-36.

Nikolau, B.J., J.B. Ohlrogge, and E.S. Wurtele. 2003. Plant biotin-containing carboxylases. *Archives of biochemistry and biophysics*. 414:211-222.

Ohlrogge, J., and J. Browse. 1995. Lipid biosynthesis. *The Plant cell*. 7:957-970.

Quanbeck, S.M., L. Brachova, A.A. Campbell, X. Guan, A. Perera, K. He, S.Y. Rhee, P. Bais, J.A. Dickerson, P. Dixon, G. Wohlgemuth, O. Fiehn, L. Barkan, I. Lange, B.M. Lange, I. Lee, D. Cortes, C. Salazar, J. Shuman, V. Shulaev, D.V. Huhman, L.W. Sumner, M.R. Roth, R. Welti, H. Ilarslan, E.S. Wurtele, and B.J. Nikolau. 2012. Metabolomics as a Hypothesis-Generating Functional Genomics Tool for the Annotation of Arabidopsis thaliana Genes of "Unknown Function". *Frontiers in plant science*. 3:15.

Quastel, J.H., and W.R. Wooldridge. 1928. Some properties of the dehydrogenating enzymes of bacteria. *The Biochemical journal*. 22:689-702.

This article is protected by copyright. All rights reserved

Author Manuscript

Reverdatto, S., V. Beilinson, and N.C. Nielsen. 1999. A multisubunit acetyl coenzyme A carboxylase from soybean. *Plant physiology*. 119:961-978.

Schmid, M., T.S. Davison, S.R. Henz, U.J. Pape, M. Demar, M. Vingron, B. Scholkopf, D. Weigel, and J.U. Lohmann. 2005. A gene expression map of Arabidopsis thaliana development. *Nature genetics*. 37:501-506.

Shannon, L.M., J. de Vellis, and J.Y. Lew. 1963. Malonic Acid Biosynthesis in Bush Bean Roots. II. Purification and Properties of Enzyme Catalyzing Oxidative Decarboxylation of Oxaloacetate. *Plant physiology*. 38:691-697.

Shockey, J.M., M.S. Fulda, and J. Browse. 2003. Arabidopsis contains a large superfamily of acyl-activating enzymes. Phylogenetic and biochemical analysis reveals a new class of acyl-coenzyme a synthetases. *Plant physiology*. 132:1065-1076.

Somerville, C.R., and W.L. Ogren. 1979. A phosphoglycolate phosphatase-deficient mutant of Arabidopsis. *Nature*. 280:833-836.

Stewart, C., Jr., C.R. Vickery, M.D. Burkart, and J.P. Noel. 2013. Confluence of structural and chemical biology: plant polyketide synthases as biocatalysts for a bio-based future. *Current opinion in plant biology*. 16:365-372.

Stumpf, D.K., and R.H. Burris. 1981. Biosynthesis of malonate in roots of soybean seedlings. *Plant physiology*. 68:992-995.

Sun, J., J. Ke, J.L. Johnson, B.J. Nikolau, and E.S. Wurtele. 1997. Biochemical and molecular biological characterization of CAC2, the Arabidopsis thaliana gene coding for the biotin carboxylase subunit of the plastidic acetyl-coenzyme A carboxylase. *Plant physiology*. 115:1371-1383.

Suzuki, H., T. Nakayama, K. Yonekura-Sakakibara, Y. Fukui, N. Nakamura, M.A. Yamaguchi, Y. Tanaka, T. Kusumi, and T. Nishino. 2002. cDNA cloning, heterologous expressions, and functional characterization of malonyl-coenzyme a:anthocyanidin 3-o-glucoside-6"-o-malonyltransferase from dahlia flowers. *Plant physiology*. 130:2142-2151.

Taguchi, G., Y. Shitchi, S. Shirasawa, H. Yamamoto, and N. Hayashida. 2005. Molecular cloning, characterization, and downregulation of an acyltransferase that catalyzes the malonylation of flavonoid and naphthol

This article is protected by copyright. All rights reserved

Author Manuscript

glucosides in tobacco cells. *The Plant journal : for cell and molecular biology*. 42:481-491.

Thelen, J.J., and J.B. Ohlrogge. 2002a. Both antisense and sense expression of biotin carboxyl carrier protein isoform 2 inactivates the plastid acetyl-coenzyme A carboxylase in Arabidopsis thaliana. *The Plant journal : for cell and molecular biology*. 32:419-431.

Thelen, J.J., and J.B. Ohlrogge. 2002b. The multisubunit acetyl-CoA carboxylase is strongly associated with the chloroplast envelope through non-ionic interactions to the carboxyltransferase subunits. *Archives of biochemistry and biophysics*. 400:245-257.

Timm, S., A. Nunes-Nesi, T. Parnik, K. Morgenthal, S. Wienkoop, O. Keerberg, W. Weckwerth, L.A. Kleczkowski, A.R. Fernie, and H. Bauwe. 2008. A cytosolic pathway for the conversion of hydroxypyruvate to glycerate during photorespiration in Arabidopsis. *The Plant cell*. 20:2848-2859.

Voll, L.M., A. Jamai, P. Renne, H. Voll, C.R. McClung, and A.P. Weber. 2006. The photorespiratory Arabidopsis shm1 mutant is deficient in SHM1. *Plant physiology*. 140:59-66.

Wada, H., D. Shintani, and J. Ohlrogge. 1997. Why do mitochondria synthesize fatty acids? Evidence for involvement in lipoic acid production. *Proceedings of the National Academy of Sciences of the United States of America*. 94:1591-1596.

Wada, M., R. Yasuno, S.W. Jordan, J.E. Cronan, Jr., and H. Wada. 2001a. Lipoic acid metabolism in Arabidopsis thaliana: cloning and characterization of a cDNA encoding lipoyltransferase. *Plant & cell physiology*. 42:650-656.

Wada, M., R. Yasuno, and H. Wada. 2001b. Identification of an Arabidopsis cDNA encoding a lipoyltransferase located in plastids. *FEBS letters*. 506:286-290.

Wang, Y., H. Chen, and O. Yu. 2014. A plant malonyl-CoA synthetase enhances lipid content and polyketide yield in yeast cells. *Applied microbiology and biotechnology*. 98:5435-5447.

Winter, D., B. Vinegar, H. Nahal, R. Ammar, G.V. Wilson, and N.J. Provart. 2007. An "Electronic Fluorescent Pictograph" browser for exploring and analyzing large-scale biological data sets. *PloS one*. 2:e718.

This article is protected by copyright. All rights reserved

Author Manuscript

Witkowski, A., J. Thweatt, and S. Smith. 2011. Mammalian ACSF3 protein is a malonyl-CoA synthetase that supplies the chain extender units for mitochondrial fatty acid synthesis. *The Journal of biological chemistry*. 286:33729-33736.

Yanai, Y., T. Kawasaki, H. Shimada, E.S. Wurtele, B.J. Nikolau, and N. Ichikawa. 1995. Genomic organization of 251 kDa acetyl-CoA carboxylase genes in Arabidopsis: tandem gene duplication has made two differentially expressed isozymes. *Plant & cell physiology*. 36:779-787.

Yasuno, R., and H. Wada. 1998. Biosynthesis of lipoic acid in Arabidopsis: cloning and characterization of the cDNA for lipoic acid synthase. *Plant physiology*. 118:935-943.

Yasuno, R., and H. Wada. 2002. The biosynthetic pathway for lipoic acid is present in plastids and mitochondria in Arabidopsis thaliana. *FEBS letters*. 517:110-114.

Author Manuscript

Figure Legends

Figure 1. *AAE13* transcript variants identified by 5' RACE analysis.

(a) Agarose gel electrophoresis analysis of the *AAE13* 5' RACE products generated from RNA isolated from the aerial organs of wild-type Arabidopsis.

(b) Molecular characterization of cloned *AAE13* 5' RACE products. Sequencing of 80 individual plasmid clones identified 5 transcript variants (*AAE13.1* to *AAE13.5*; the number of each transcript variant recovered is shown), and their representative molecular structures are mapped relative to the *AAE13* (AT3G16170) gene model (5' UTR and *AAE13* CDS) that was previously characterized (Chen et al., 2011). The first 2 exons each contain an "ATG" translational start codon (Exon1 "ATG" and Exon2 "ATG").

This article is protected by copyright. All rights reserved

Figure 2. Subcellular localization of *AAE13*-encoded proteins determined with GFP-tagged transgenic Arabidopsis plants.

(a) Confocal fluorescence micrographs of roots of non-transgenic wild-type (WT) control plants (Row 1); transgenic line carrying the P_{35S}*::AAE13*$_{258}$*-GFP* transgene (Row 2); and transgenic line carrying the P_{35S}*::GFP* control transgene (Row 3). Fluorescence signals were imaged for GFP (Column 1), MitoTracker Orange (Column 2), and the merged images of GFP and MitoTracker Orange (Column 3).

(b) Confocal fluorescence micrographs of mesophyll cells of non-transgenic WT control plants (Row 1); transgenic line carrying the P_{35S}*::AAE13*$_{258}$*-GFP* transgene (Row 2); and transgenic line carrying the P_{35S}*::GFP* control transgene (Row 3). Fluorescence signals were imaged for GFP (Column 1), chlorophyll autofluorescence (Column 2), and the merged images of GFP and chlorophyll autofluorescence (Column 3).

Figure 3. Quantitative RT-PCR analysis of the expression of the *AAE13*-derived mRNAs in different Arabidopsis organs. Results are the mean of 3 biological replicates ± standard error (SE), and are presented as normalized values relative to the expression of the *Actin-2* gene (see Experimental Procedures). Integrated sum of transcripts *AAE13.1*, *AAE13.2*, *AAE13.3*, *AAE13.4* and *AAE13.5*, which encode both the mitochondrially and cytosolically located AAE13 proteins (■), and integrated sum of transcripts *AAE13.1* and *AAE13.2* that encode mitochondrially located AAE13 protein (□). Numbers on the *x*-axis represent day after imbibition (DAI) for each specific sample.

Figure 4. Transgenic complementation of the *aae13-1* mutant.

(a) Molecular representations of the structures of the 4 transgenes used to transform the wild-type (WT) plants and *aae13-1* mutant line.

(b) Representative images of the morphological appearance of each of 5 transgenic lines.

This article is protected by copyright. All rights reserved

Author Manuscript

Figure 5. Chemical complementation of the *aae13-1* mutant lines. The wild-type (WT) plants, *aae13-1* mutant line, and *aae13-1* mutant carrying the P_{AAE13}*::AAE13* transgene, grown in ambient air or in the 1% CO_2 atmosphere.

Figure 6. Protein lipoylation status in the aerial organs of the *aae13-1* mutant lines. SDS-PAGE analysis and Western blot analysis of extracts from the aerial organs of 16 DAI plants grown in the 1% CO_2 atmosphere. Plant genotypes were: the wild-type (WT) plants, *aae13-1* mutant line, and *aae13-1* mutant carrying the P_{AAE13}*::AAE13* transgenes.

(a) Coomassie Brilliant Blue-stained SDS-PAGE analysis.

(b) Western blot analysis of the H protein of GDC detected with anti H-protein antibodies, and the lipoylation status of the H-protein and other indicated lipoylated proteins detected with anti-lipoic acid antibodies.

Figure 7. Metabolic alterations in the *aae13-1* mutant. The *aae13-1* mutant line and wild-type (WT) plants were grown either in ambient air (●) or in the 1% CO_2 atmosphere (O). The *y*-axis plots individual metabolites. The *x*-axis plots log_2-transformed relative ratio of abundance of each metabolite in the *aae13-1* mutant sample normalized to the same metabolite in the WT control sample. Results are presented as mean ± SE (See Experimental Procedures).

Author Manuscript

This article is protected by copyright. All rights reserved

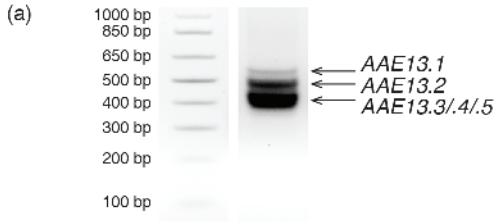

(b)

Transcript Variants	Number of Plasmids
AAE13.1	4
AAE13.2	17
AAE13.3	24
AAE13.4	25
AAE13.5	12

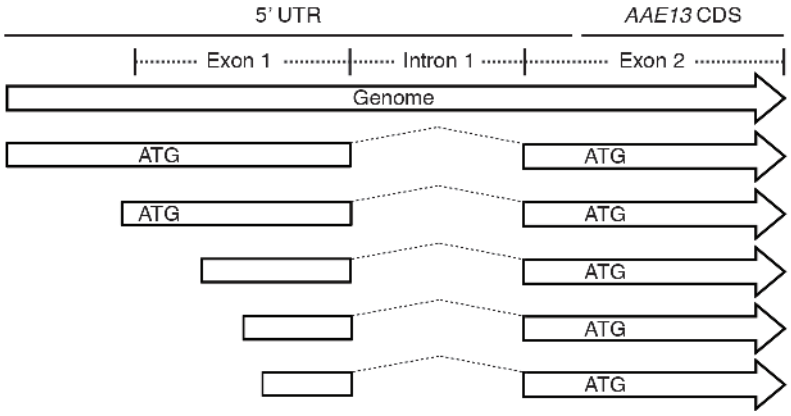

tpj_13130_f1.tif

Author Manuscript

This article is protected by copyright. All rights reserved

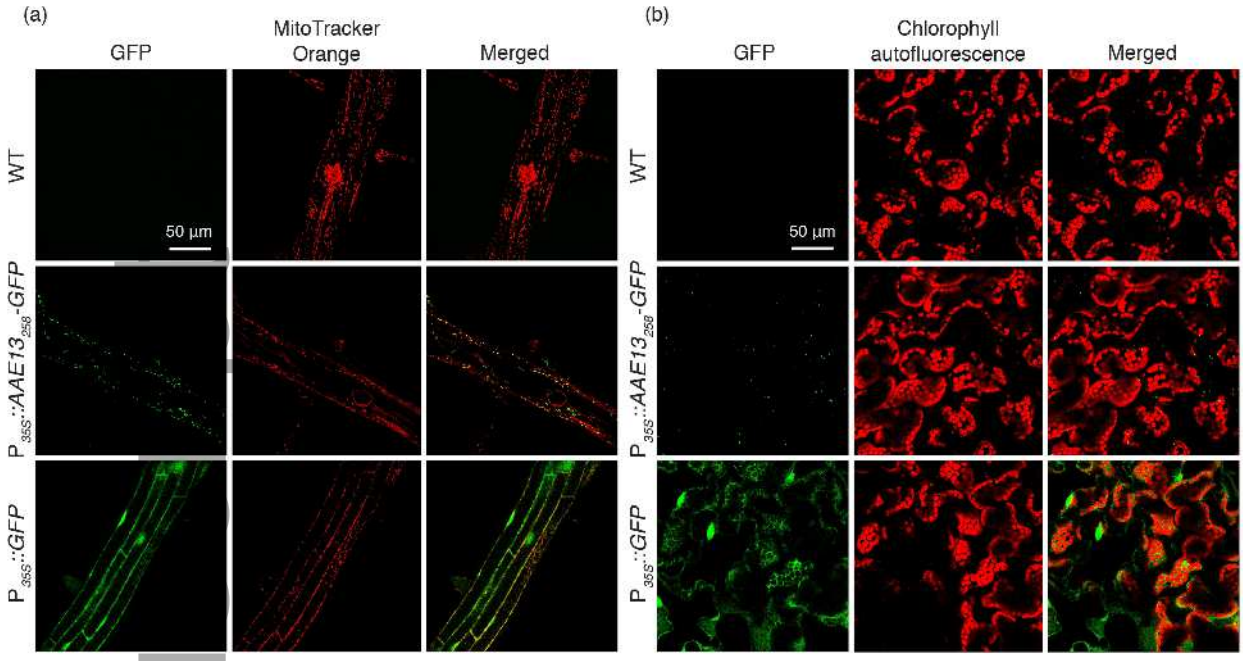

tpj_13130_f2.tif

Author Manuscript

This article is protected by copyright. All rights reserved

Author Manuscript

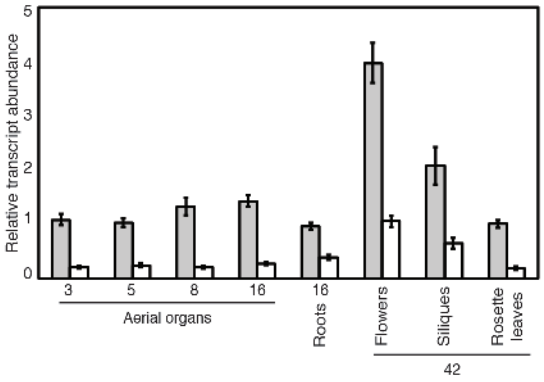

tpj_13130_f3.tif

This article is protected by copyright. All rights reserved

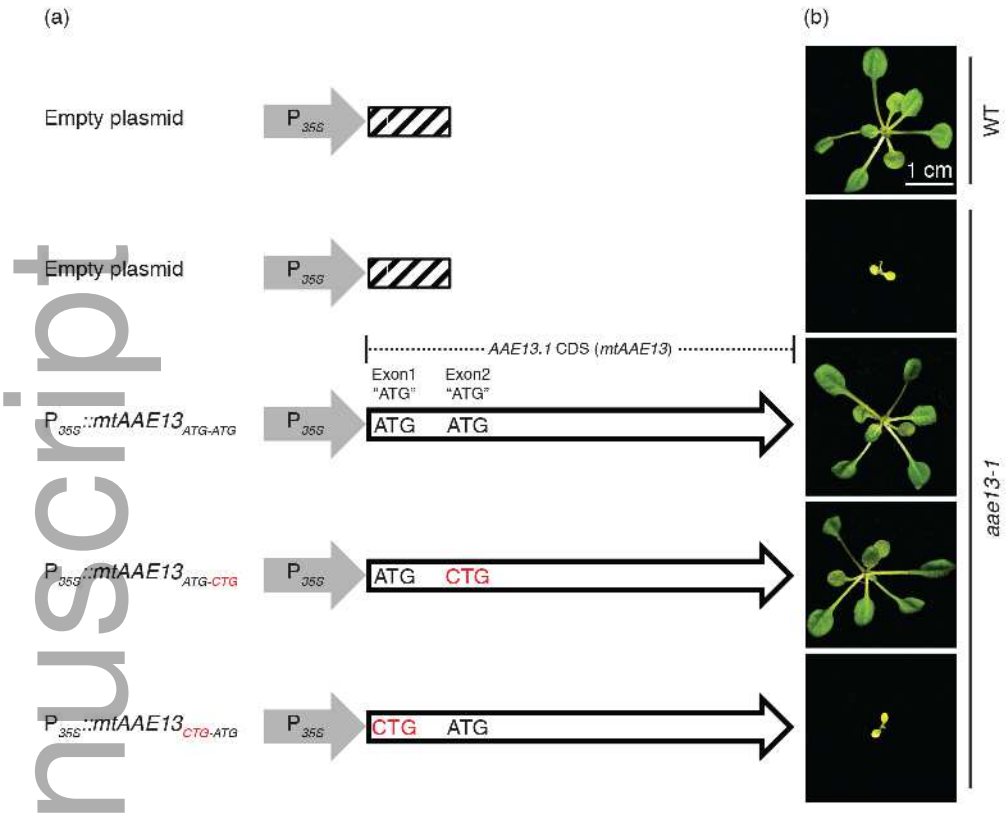

tpj_13130_f4.tif

Author Manuscript

This article is protected by copyright. All rights reserved

Author Manuscript

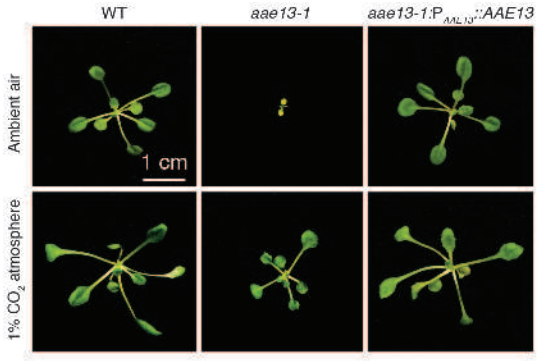

tpj_13130_f5.tif

This article is protected by copyright. All rights reserved

Author Manuscript

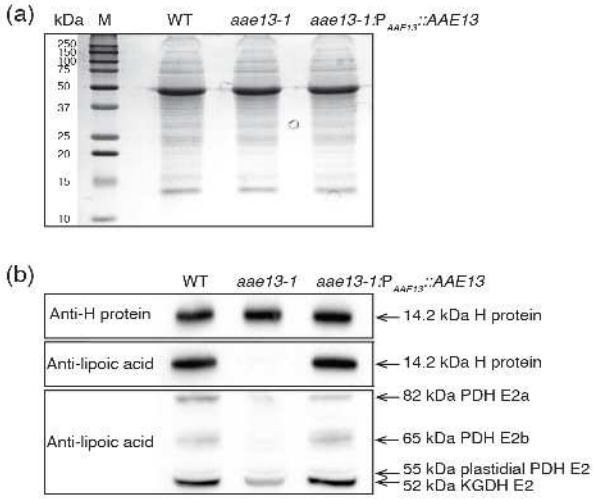

tpj_13130_f6.tif

This article is protected by copyright. All rights reserved

Author Manuscript

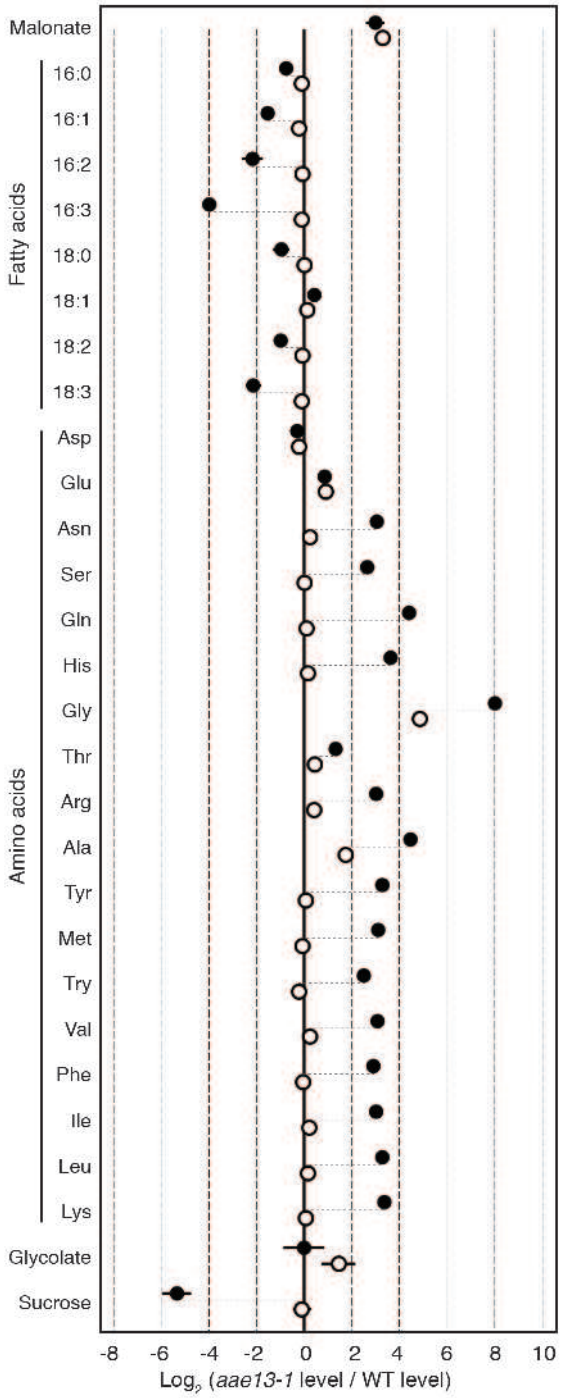

tpj_13130_f7.tif

This article is protected by copyright. All rights reserved